


 Cite this: *RSC Adv.*, 2020, 10, 27173

# Evaluation of biosynthesis parameters, stability and biological activities of silver nanoparticles synthesized by *Cornus Officinalis* extract under 365 nm UV radiation†

 Yinghui Wang,<sup>†a</sup> Simin Wei,<sup>†\*b</sup> Kang Wang,<sup>a</sup> Zhe Wang,<sup>b</sup> Jinwei Duan,<sup>a</sup> Lin Cui,<sup>a</sup> Huayu Zheng,<sup>a</sup> Ying Wang<sup>a</sup> and Shanshan Wang<sup>a</sup>

Since silver nanoparticles (AgNPs) synthesized by using plant extracts revealed varied biological activities, the green synthesis of AgNPs has attracted considerable attention. Although the green synthesis of AgNPs have been accomplished by using the extracts of *Cornus Officinalis*, which is a traditional Chinese medicine and exhibits a wide spectrum of phytochemicals. The effects of biosynthesis parameters on reducing reaction, stability and more broad biological activities of so-prepared AgNPs did not been evaluated. In this paper, we firstly assessed the effects of UV radiation, pH, material proportion and radiation times on the green synthesis of AgNPs under 365 nm UV radiation by UV-visible spectrum and dynamic light scattering (DLS) analysis. The results showed that UV radiation could accelerate the formation of AgNPs and influence the average size below pH 7.0, and the size of so-prepared AgNPs were sensitive to the pH and material proportion, but no obvious changes to UV radiation times, offering a size-controlled synthetic method for AgNPs. The further X-ray diffraction (XRD), transmission electron microscopy (TEM) and DLS studies showed AgNPs synthesized at pH 7.0, extract: AgNO<sub>3</sub> = 1 : 1 and after 4 h UV radiation were a face-centered cubic (fcc) structure and both spherical and polygonal in shape with average particle size of 64.5 ± 0.3 nm existed in a monodispersed form. Subsequently, the stability of AgNPs was analyzed by zeta potential (−24.8 mV) and the average size measurement after 30 days storage (63.3 ± 0.4 nm), revealing a high degree of stability. Lastly, the investigation of biological activities showed that the biosynthesized AgNPs had potent antioxidant activity, antimicrobial activity against both *S. aureus* and *E. coli* as well as anticancer activity against HCT116 and HepG2 cell lines but negligible cytotoxicity against SW620. And the internalization of biosynthesized AgNPs inside the bacterial cell was evaluated by flow cytometric analysis, where the SSC values have significant increase after treating with nanoparticles. These results confirmed that the biosynthesis parameters on the green synthesis of AgNPs by using *Cornus Officinalis* extract also played pivotal roles and so-prepared AgNPs would be useful for the development of new alternative antioxidant, antimicrobial and anticancer agents in biomedicine.

Received 20th May 2020

Accepted 13th July 2020

DOI: 10.1039/d0ra04482b

[rsc.li/rsc-advances](http://rsc.li/rsc-advances)

## Introduction

Silver nanoparticles (AgNPs) have attracted tremendous attention from analysts due to various applications in many fields of science such as biomedicine, pharmaceuticals, cosmetics,

catalysis, textiles and optics.<sup>1–5</sup> Especially for biomedical purposes, they have been widely used in antimicrobial agents, molecular imaging, drug delivery, biomedical sensing, and even cancer photodynamic therapy.<sup>5–7</sup> Although the synthesis of AgNPs could be easily achieved with high yield by various methods, such as physical, photochemical, electrochemical and many others,<sup>4,8</sup> simultaneously there have some limitations in these methods like significant toxic effects associated with AgNPs exposure *in vitro* and *in vivo* studies. To overcome these negative impacts of above mentioned synthetic methods, the new green, eco-friendly synthetic approaches by using biological resources such as plants, biopolymers and microorganisms as reducing and capping agents have been developed.<sup>9–13</sup> Since plant-based synthesis can be improved easily, less bio-

<sup>a</sup>College of Science, Chang'an University, Xi'an 710064, China

<sup>b</sup>Shaanxi Collaborative Innovation Center of Chinese Medicine Resources Industrialization, State Key Laboratory of Research & Development of Characteristic Qin Medicine Resources, Shaanxi Innovative Drug Research Center, Shaanxi University of Chinese Medicine, Xi'an 712083, China. E-mail: weisimin@iccas.ac.cn

† Electronic supplementary information (ESI) available. See DOI: 10.1039/d0ra04482b

‡ These authors contributed equally.



threatening and do not include the step of cell culture growth, it is generally adopted more frequently compared to these methods by using microorganisms and biopolymers.

In the process of plant-based synthesis, phytochemicals including terpenoids, flavones, ketones, aldehydes, amides, carboxylic acids, carbohydrates, proteins, and vitamins *etc.*, play an important role,<sup>11,12,14</sup> where they act as not only the reducing agents but also capping agents. These capping agents are advantageous over as they prevent the nanoparticles from the agglomeration, reduce the toxicity and improve the biomedical activities. A synergistic effect of metal nanoparticles and these capped molecules are anticipated when these coating agents themselves show biological activities. To date, several plant parts including the seeds, stem, fruits, root and leaf have been employed for synthesizing different sizes and shapes of AgNPs such as *Iresine herbstii* leaf,<sup>15</sup> *Piper betle* leaf,<sup>16</sup> oak fruit hull,<sup>17</sup> *Nelumbo nucifera* leaf and root,<sup>18,19</sup> *Neem* leaf,<sup>20</sup> *Eriobotrya japonica* leaf,<sup>21</sup> *Coffea arabica* seed<sup>22</sup> and so on. Otherwise, we also utilized the berry extract of *Sea Buckthorn* to obtain the AgNPs with superior antioxidation and anticancer activity.<sup>23</sup>

*Cornus Officinalis* (Scheme 1) is a traditional Chinese herbal medicine for the treatment of diabetes, cancer and shock. The phytochemical studies have revealed that the extract of *Cornus Officinalis* contains more than 150 compounds including flavonoids, structurally diverse iridoid glycosides, anthocyanins, saccharides and tannins.<sup>24</sup> Due to the wide range of fascinating bioactivities like anti-inflammatory, anti-oxidative and anti-neoplastic activities, some kind of these compounds have roused lots of interests from analysts.<sup>25–28</sup> Although He and his coworkers have used the extracts of *Cornus Officinalis* for the green synthesis of AgNPs at ambient temperature.<sup>29</sup> The effects of biosynthesis parameters for the reducing reaction and the stability of biosynthesized AgNPs are still unknown, which have strong influence on the size, morphology, stability, and physicochemical properties of metal nanoparticles.<sup>16,30,31</sup> On the

other hand, considering the broad biological activities of *Cornus Officinalis*, the AgNPs prepared by using its extracts should possess various pharmacological effects. However, only the cytotoxicity activities against human cell lines PC-3, HepG2 and SGC-7901 were evaluated. Obviously, further investigation on the green synthesis of AgNPs by using *Cornus Officinalis* should be proceeded.

Herein, we were motivated to systematically evaluate the effects of biosynthesis parameters on reducing reaction, stability and biological activities of AgNPs synthesized by using *Cornus Officinalis* extract under 365 nm UV radiation at ambient temperatures. Firstly, the effects of UV radiation and biosynthesis parameters, such as pH, material proportion and radiation time were assessed by using UV-visible spectrum and dynamic light scattering achieving size-controlled AgNPs. Then, the shape, size, surface properties and the stability of so-prepared AgNPs were confirmed by further X-ray diffraction (XRD), transmission electron microscopy (TEM) and dynamic light scattering (DLS) characterization. Lastly, by calculating the radical scavenging rate for DPPH, the cell viabilities for three cell lines, and the minimum inhibition concentration (MIC) for *E. coli* and *S. aureus*, the biological activities of biosynthesized AgNPs were evaluated systematically. Also, the values of side scatter (SSC) was obtained for assessing the AgNPs internalization in bacterial cells. These results reveals that the biosynthesis parameters on the green synthesis of AgNPs by using *Cornus Officinalis* extract also played important roles in the size and morphology and so-prepared AgNPs could be a promising candidate for antioxidant, antimicrobial and anticancer drugs.

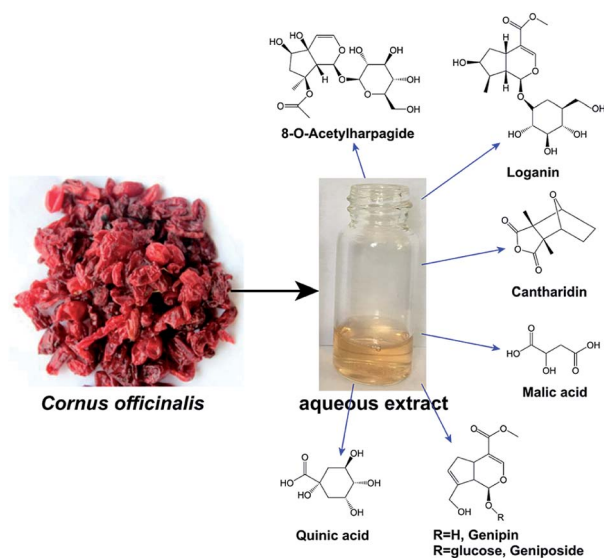
## Experimental

### Chemicals

*Cornus Officinalis* was bought from Shaanxi Sciendan Pharmaceutical co., Ltd. (Xi'an, China). Silver nitrate (AgNO<sub>3</sub>, 99.8%), tryptone, sodium chloride, yeast powder and agar powder were purchased from Chron Chemicals Co., Ltd. (Chengdou, China). 1,1-diphenyl-2-picrylhydrazulin (DPPH, >99.5%) were purchased from Shanghai Aladdin Bio-Chem Technology Co., LTD. 3-(4,5-Dimethyl-2-thiazolyl)-2,5-diphenyl-2H-tetrazolium bromine (MTT) and dimethyl sulfoxide (DMSO) were purchased from Solarbio Science & Technology Co. Ltd. (Beijing, China). Other reagents were purchased from Sigma Aldrich. Human colorectal cancer HCT116 and SW620, human hepatoma cancer HepG2 cell lines were purchased from the cell repository of the Chinese Academy of Sciences (Shanghai, China). All solutions were prepared in ultrapure Milli-Q water. All chemicals were analytical grade and used without further purification.

### Synthesis of silver nanoparticles

The dried fruit of *Cornus Officinalis* (5.0 g, powder) was sonicated for 4 h with 100.0 mL deionized water. The extract was then filtered and stored in 4 °C for further studies. Synthesis of AgNPs was performed by mixing 5.0 mL aqueous extract and 5.0 mL 10 mM AgNO<sub>3</sub> under 365 UV radiation at ambient temperatures for 4 h. Thereafter, the mixture was centrifuged



Scheme 1 Some biologically active compounds from *Cornus officinalis* extract.



for 30 min at 10 000 rpm to purify the AgNPs. The resulted precipitate was washed by deionized water three times and then lyophilized 12 h. The effects of pH values of aqueous extract (3.0, 4.0, 5.0, 6.0 and 7.0), the ratio of the reactants (1 : 1, 1 : 2, 1 : 3, 1 : 5, 1 : 10) and the UV radiation time were evaluated as the procedures mentioned above.

### Characterization of silver nanoparticles

By using UV-Vis spectrophotometer (UV-2600, Japan), the formation of AgNPs synthesized by *Cornus Officinalis* extract under 365 nm UV radiation was periodically monitored by collecting the spectral range from 200 to 800 nm. The morphology of the AgNPs was characterized using transmission electron microscopy (TEM) images (JEM-2010, Japan) at 120 kV. A drop of water solution containing AgNPs was put onto a carbon-coated copper grid and dried completely. The crystalline phase of the AgNPs was analyzed by a Shimadzu XRD-7000S X-ray diffractometer (Japan). The diffracted intensities were recorded from 20° to 80° 2θ angle at a scanning rate of 5° per minutes. The tube current and voltage are 30 mA and 40 kV, respectively. The surface loads and average sizes of AgNPs were measured by Malvern Zetasizer Nanoseries (ZEN 3600, Malvern, UK). Zeta potential was evaluated at 25 °C, at an angle of 17 °C and 78.5 dielectric constant. Electrical field was operated to 15 V cm<sup>-1</sup>. Data obtained were analyzed using Zetasizer software.

### Antioxidant activity of silver nanoparticles

DPPH radical scavenging activity of the AgNPs was performed on the basis of bleaching of the 1,1-diphenyl-2-picrylhydrazulin (DPPH) absorbance at 517 nm in ethanol. DPPH was used as a reagent in the spectrophotometric assay. Serial concentrations (0–100.0 μg mL<sup>-1</sup>) of AgNPs (1 mL) synthesized by *Cornus Officinalis* extract were prepared and added to 1 mL DPPH solution (2.5 mg mL<sup>-1</sup>). The reaction mixtures were vigorously shaken and incubated for 30 minutes in dark at room temperature, followed by measuring the absorbance at 517 nm. Negative control group was prepared without AgNPs. The radical scavenging rate was calculated according to the given formula:

$$\text{Scavenging rate (\%)} = [1 - (A_1 - A_2)/A_0] \times 100\%$$

where A<sub>0</sub> is the absorbance of the DPPH and ultrapure water at 517 nm, A<sub>1</sub> is the absorbance of DPPH and AgNPs at 517 nm, A<sub>2</sub> is the absorbance of ethanol and AgNPs at 517 nm.

### Antimicrobial activity of silver nanoparticles

To test the antibacterial activity of the AgNPs synthesized by *Cornus Officinalis* extract, the growth inhibition studies against both Gram positive (*S. aureus*) and Gram negative (*E. coli*) bacteria were conducted in Luria–Bertani (LB) broth media. The experiments were carried out using previously reported methods with some modifications.<sup>32</sup> For growth inhibition studies, 96-well plates, each containing 50 μL LB broth media and the desired amount of AgNPs, were inoculated with 50 μL of the freshly prepared bacterial suspension in order to maintain

initial bacterial concentration in the same range in the well. The 96-well plates were then incubated in a rotary shaker at 160 rpm at 37 °C. Bacterial growth was then monitored every hour for 24 h by measuring the increase in absorbance at 600 nm. The experiments also included a control well containing only media and bacteria devoid of AgNPs.

### Internalization of silver nanoparticles

According to the method of Suzuki *et al.*,<sup>33</sup> we performed the flow cytometric analysis for the assessment of AgNPs internalization in bacterial cells (*E. coli* and *S. aureus*) using light scattering principles. In brief, the bacterial were seeded in 96-well culture plates and exposed to 5.0 μg mL<sup>-1</sup> concentration of AgNPs for 12 h. After indicated incubation period, bacterial cells were harvested and resuspended in 1.0 mL PBS. Analysis was made by using flow cytometer.

### Anticancer activity of silver nanoparticles

Human colorectal cancer HCT116 and SW620, human hepatoma cancer HepG2 cell lines were cultured at 37 °C in a humidified atmosphere containing 5% CO<sub>2</sub> and grown continuously in DMEM medium supplemented with 10% heat inactivated fetal bovine serum (FBS). Cells were plated out in flat bottom 96-well plates at a density of 1 × 10<sup>4</sup> cells per well and allowed to attach for 24 h. After sucking up the supernatant, the different concentrations of AgNPs (0.8–100.0 μg mL<sup>-1</sup>) were added into 96-well plates. The cells were then incubated at 37 °C in an atmosphere of 5% CO<sub>2</sub> for 24 h followed by an MTT assay. 20 μL Thiazolyl Blue Tetrazolium Bromide (MTT) (5 mg mL<sup>-1</sup>; Solarbio) and 150 μL DMEM media were freshly added to each well. After incubation for 4 h, the media was gently removed. The formed formazan crystals were dissolved in 150 μL DMSO, subsequently the absorbance was measured with a plate reader (Perkin Elmer) at 490 nm. The cell viability was calculated according to the given formula:

$$\text{Cell viability (\%)} = (A - A_b)/(A_0 - A_b) \times 100\%$$

where A is the absorbance of the sample, A<sub>b</sub> is the bleaching absorbance without the sample, and A<sub>0</sub> is the absorbance value of the control.

## Results and discussion

### The biosynthesis of AgNPs and the effects of biosynthesis parameters

AgNPs were initially prepared by reducing Ag<sup>+</sup> in 5.0 mL of 10 mM AgNO<sub>3</sub> solution with 5.0 mL primary *Cornus Officinalis* extract (pH 3.0) without any auxiliary means at ambient temperature. The mixed solution of AgNO<sub>3</sub> and primary *Cornus Officinalis* extract did not have any minor changes in color until a few hours later, suggesting a weak reducibility of primary *Cornus Officinalis* extract. Based upon previous studies,<sup>34</sup> the phytochemicals of *Cornus Officinalis* extract have strong absorbance in UV region, indicating that they could absorb the UV. These compounds absorbing UV tend to populate in the excited



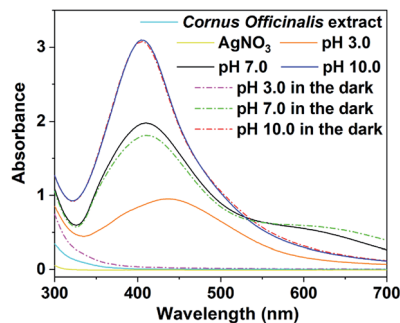


Fig. 1 UV-Vis spectra of the mixture after 1 h reaction between *Cornus officinalis* extract and AgNO<sub>3</sub> with/without 365 nm UV radiation at different pH.

state like the singlet and triplet excited state, which have been confirmed to loss of electron easier meaning the more reducibility.<sup>35</sup> Thus, the mixture of AgNO<sub>3</sub> and primary *Cornus Officinalis* extract were radiated by 365 nm UV, where the absorbance of *Cornus Officinalis* extract have negligible changes before and after 365 nm UV radiation (Fig. S1†). The color of mixed solution turned yellow to dark brown after 1 h UV radiation (Fig. S2†), indicating that AgNPs have been formed. The 365 nm UV seems to promote the formation of AgNPs. Since the AgNPs showed obvious surface plasmon resonance (SPR) band at 400–500 nm, the formation of AgNPs were further confirmed by UV-Vis spectroscopy measurement, where the *Cornus Officinalis* extract and AgNO<sub>3</sub> had negligible absorbance. Fig. 1 displays the UV-Vis spectroscopy of the mixture with/without UV radiation. The spectrum clearly displays a strong absorption band peaking at 437 nm under 365 nm UV radiation, but no obvious absorbance without UV radiation. This spectrum features of the mixture under 365 nm UV radiation essentially resemble previous studies about the SPR peak of AgNPs, further confirming the formation of AgNPs and the important roles of UV radiation in green synthesis. This result is consistent with the observation in color by naked eyes. It should be noticed that the spectrum obtained under UV radiation also have some differences. The resonant absorption of photons by so-prepared AgNPs were at lower energy as that obtained by He<sup>36</sup> and Kaur<sup>30</sup> indicating a bigger size of AgNPs. To confirm the suppose, the average size of biosynthesized AgNPs ( $116.9 \pm 1.7$  nm) was measured by dynamic light scattering (DLS) method as shown in Fig. 2B and Table S1.† The result of DLS is consistent with the observation from UV spectroscopy.

Studies have shown that the biosynthesis parameters, such as pH of extract, material proportion and reaction time would have strong influence on the size, morphology, stability, and physicochemical properties of metal nanoparticles,<sup>16,30,31</sup> which play pivotal roles in controlling the physical, chemical, optical, and electronic properties of these nanoscopic materials. As He and his coworkers have biosynthesized the AgNPs with high yield by using *Cornus officinalis* extract at pH 8.0 in the dark,<sup>29</sup> we firstly tested the effects of UV radiation at different pH (Fig. 1). The result of UV-Vis spectroscopy measurement clearly showed that below pH 7.0, the UV radiation could accelerate the

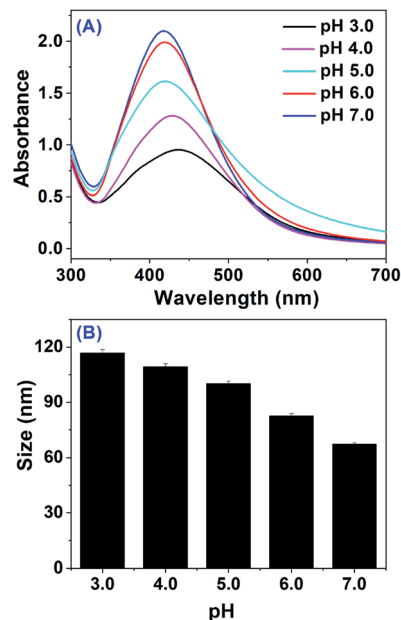


Fig. 2 (A) UV-Vis spectra of the mixture after 1 h reaction between *Cornus officinalis* extract and AgNO<sub>3</sub> under 365 nm UV radiation at different pH; (B) the size of AgNPs obtaining at (A).

formation of AgNPs. On the other hand, we also noticed that UV radiation could make the average size of synthesized AgNPs (61.8 nm) smaller than that prepared at pH 7.0 without UV radiation (71.6 nm). But at pH 10.0, neither the formation yield nor the average size suffered from 365 nm UV radiation. The average size synthesized at pH 10.0 with and without UV radiation were 41.2 and 40.8 nm, respectively. Considering the weak effect of UV radiation on the formation of AgNPs at alkaline, we would then mainly discuss the pH effect below 7.0.

As shown in Fig. 2A, with pH increasing to 5.0, the SPR peak of AgNPs at 437 nm sharply increases accompanying with band shift to 417 nm. The 417 nm band then decays gradually until pH 7.0 with a slightly band shift to 413 nm. The variation of SPR band intensity should reflect the formation amounts of AgNPs by *Cornus Officinalis* extract under UV radiation. This suggested that with the pH increases from 3.0 to 5.0, the formation amounts of AgNPs sharply increased and yet when the pH successively rose to 7.0, the formation amounts of AgNPs decreased. The spectral evolution may originate from the photochemical reaction among the active compounds in *Cornus Officinalis* extract above pH 5.0. The blue shift of the SPR peak from 437 nm to 413 nm with the increased pH indicated that smaller size particles were formed at high pH value. This is in accordance with previous results obtained by Sathishkumar<sup>32</sup> and Heydari.<sup>17</sup> DLS measurements of the average size of biosynthesized AgNPs reveal a reduced size from  $116.9 \pm 1.7$  to  $67.5 \pm 0.7$  nm with the increased pH further confirmed the UV spectral observation. We also noticed that the SPR peak showed broad distribution at pH 7.0, indicating the formation of anisotropic particles, which was confirmed by following TEM characterization.



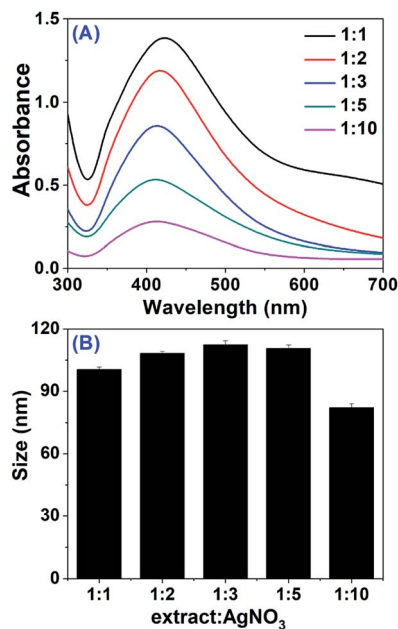


Fig. 3 (A) UV-Vis spectra of the mixtures after 1 h reaction between *Cornus officinalis* extract and AgNO<sub>3</sub> under 365 nm UV radiation at different proportions; (B) the size of AgNPs obtaining at (A).

Then, the effect of materials proportion of *Cornus officinalis* extract and AgNO<sub>3</sub> were evaluated. The UV-Vis spectra of the mixed solution of *Cornus officinalis* extract (pH 7.0) and AgNO<sub>3</sub> at different proportions after 1 h UV radiation at ambient temperature were obtained as shown in Fig. 3A, where the volume of AgNO<sub>3</sub> (5.0 mL) and mixture (10.0 mL) kept in constant. When the ratio of *Cornus officinalis* extract to AgNO<sub>3</sub> is 1 : 10, a relatively weak band with maximum absorbance at 403 nm was observed. With the increase in material proportion of reaction mixture to 1 : 1, the peak intensity increased continuously, indicating an enhanced production yield of AgNPs. The increased yield of biosynthesized AgNPs at high dose of *Cornus officinalis* extract may arise from the more active compounds in the mixture solution. Meanwhile, on increasing dose of *Cornus officinalis* extract, a red shift from 403 to 413 nm was observed in the absorption spectra, indicating a increased size for AgNPs. Interestingly, the measured average sizes by DLS at different dose of *Cornus officinalis* extract (Fig. 3B and Table S2<sup>†</sup>) were maximum at the proportion 1 : 3, which is proximate to the size obtaining at 1 : 5. We noticed that when the dose of *Cornus officinalis* extract rose to 1 : 5, a flat absorbance above 550 nm occurred and with the dose of *Cornus officinalis* extract increasing, this flat absorbance enhanced consecutively. This new flat absorbance may result from the products of photochemistry reactions, which may make the SPR peak shift to red. Thus, we observed the red shift of AgNPs SPR band with the enhanced dose of *Cornus officinalis* extract. For the size distribution of AgNPs at different dose, we speculated which may result from photochemistry reactions and its products.

Lastly, we tested the effect of UV radiation time on both the biosynthesis and size of AgNPs. Fig. 4A shows the absorption

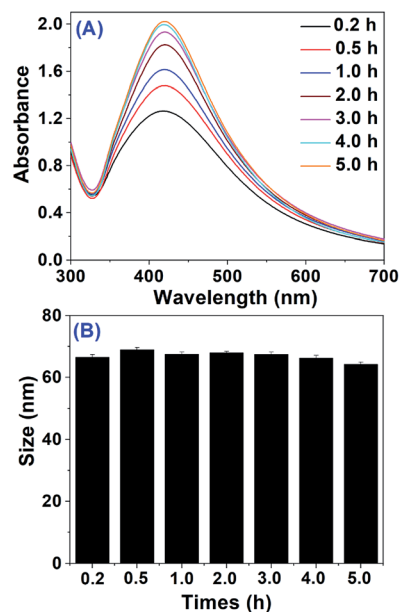


Fig. 4 (A) UV-Vis spectra of the mixture after the reaction between *Cornus officinalis* aqueous extract and AgNO<sub>3</sub> under 365 nm UV radiation at different times; (B) the size of AgNPs obtaining (A).

spectra of AgNPs obtained from the mixture of 5.0 mL *Cornus officinalis* extract (pH 7.0) and 5.0 mL AgNO<sub>3</sub> recorded at different radiation times. The characteristic SPR band of AgNPs was clearly observed at 413 nm after 0.2 h UV radiation at ambient temperatures, indicating the AgNPs could be formed within 0.2 h. It was also observed that the absorption intensity increased steadily as a function of reaction time and reached a maximum after 4 h, suggesting an enhancement of the bio-synthesized AgNPs and the reduction reaction almost completed within 4 h. The UV-Vis spectra displayed no obvious band shift with the increased reaction time, meaning the almost similar size of so-prepared AgNPs after different radiation times. The DLS measurements of AgNPs showed that the size distributed in the range of  $64.2 \pm 0.8$  to  $68.9 \pm 0.7$  nm (Fig. 4B and Table S3<sup>†</sup>) consistent with the observation from UV-Vis spectra. In order to get more products with small size for further biological study, AgNPs were prepared by using 5.0 mL of 10 mM AgNO<sub>3</sub> and 5.0 mL *Cornus officinalis* extract (pH 7.0) after UV radiation of the reaction mixture for 4 h.

### Characterization of biosynthesized AgNPs

We performed a serial of experiments like XRD, TEM and DLS for the characterizations of biosynthesized AgNPs to confirm proper synthesis, size, shape and surface property. The XRD pattern of biosynthesized AgNPs by *Cornus officinalis* extract was recorded in the range of 30 to 80 at  $2\theta$  angles as shown in Fig. 5A. The biosynthesized AgNPs showed obvious Bragg's diffraction peaks at  $2\theta$  angle of  $37.9^\circ$ ,  $44.1^\circ$ ,  $64.4^\circ$  and  $77.4^\circ$  corresponding to (111), (200), (220), and (311) facets, respectively. The XRD pattern of biosynthesized AgNPs matched well with the standard diffraction lines of cubic Ag (JCPDS, 04-0783), indicating a face-centered cubic (fcc) crystalline structure. This



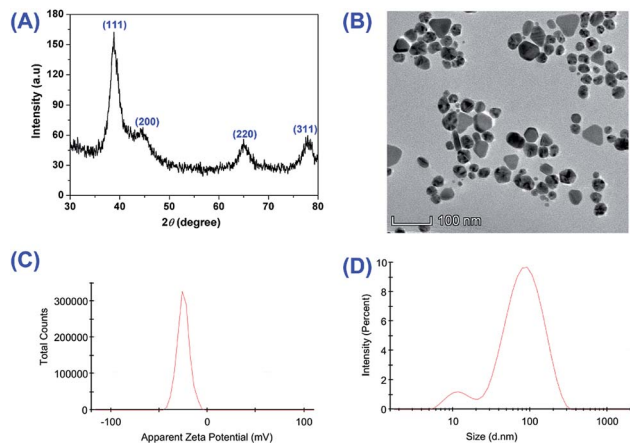


Fig. 5 (A) XRD; (B) TEM image; (C) zeta potential and (D) the size of biosynthesized AgNPs.

is consistent with the results obtained by He and his coworkers using *Cornus officinalis* extract at pH 8.0.<sup>29</sup> The result of XRD clearly displays the presence of crystalline structure of AgNPs and confirms further that the *Cornus officinalis* extract (pH 7.0) could reduce the  $\text{Ag}^+$  to AgNPs under 365 nm UV radiation.

TEM images (Fig. 5B) showed that the biosynthesized AgNPs were both spherical and polyhedral in shape consistent with the UV spectrum observation. Almost all of the particles were monodisperse. The size for the biosynthesized AgNPs were roughly in the range of 50–60 nm. The average size obtained by DLS was approximately  $64.5 \pm 0.3$  nm (Fig. 5D), basically in accordance with the TEM result. Here, the morphology and size of AgNPs obtained by our group showed obvious difference with He and his coworkers,<sup>29</sup> where the biosynthesized AgNPs were spherical in shape with average size  $12.8 \pm 3.5$  nm. These big differences in morphology and size may originate from the lower pH and UV radiation.

We also measured the zeta potential of the biosynthesized AgNPs to evaluate the surface state of the nanoparticles and predict the long-term stability. Based upon previous studies,<sup>17,37</sup> if the zeta potential of nanoparticles is outside the interval of  $-25.0$  to  $+25.0$  mV, they would have high degrees of stability. In parallel, the nanoparticles with zeta potential between the interval would have interparticle attractions and eventually lead to the aggregation of nanoparticles. As shown in Fig. 5C, the zeta potential of biosynthesized AgNPs by *Cornus officinalis* extract was  $-24.8$  mV approximating to boundary of  $-25.0$  mV, indicating a high degree of stability. Practically, the average size of biosynthesized AgNPs ( $63.3 \pm 0.4$  nm) did not have any apparent changes after 30 days (Fig. S3†). The negative zeta potential also suggested that the electronegative agents in the *Cornus officinalis* extract were attached to the surface of biosynthesized AgNPs. To further illuminate the possible agents capping in the surface of AgNPs, we performed the LC-MS analysis. Many compounds were found within our *Cornus officinalis* extract. The top 10 active compounds were loganin, quinic acid, 8-*O*-acetylharpagide, cantharidin, malic acid, genipin, geniposide, asiatic acid, 2-methoxycinnamic acid, 5-hydroxymethylfurfural and triptonide (Scheme 1 and Table

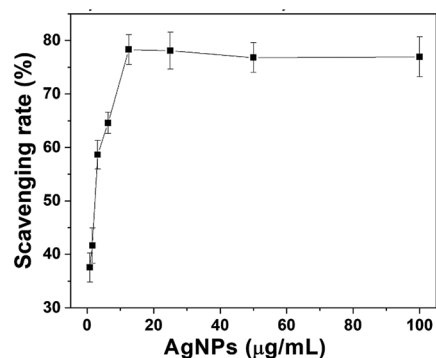


Fig. 6 Free radical scavenging rate of biosynthesized AgNPs against DPPH.

S4†). The polydispersity index (PDI) was also obtained which was an important parameter for assessing the characteristics of nanoparticles.<sup>37</sup> It has been reported that the sample with PDI values lower than 0.3 would exist in monodisperse form. Here, the PDI of AgNPs biosynthesized by *Cornus officinalis* extract was  $0.250 \pm 0.008$ , meaning the superior monodispersity in coincidence with the observation from TEM image.

#### Antioxidant activities of biosynthesized AgNPs

Based upon previous chemical researches and our LC-MS analysis, *Cornus officinalis* contained a high content of triterpenoids, iridoids, flavonoids, tannins, organic acids and polysaccharides in the fruit, where some of these bioactive compounds and their modified nanoparticles had powerful antioxidant activity and could scavenge a variety of free radicals.<sup>38,39</sup> As the AgNPs were capped by the bioactive constituents of *Cornus officinalis* extract, it was anticipated that the AgNPs biosynthesized by *Cornus officinalis* extract would also have powerful antioxidant activity. To evaluate the antioxidant activity of biosynthesized AgNPs, the DPPH method was carried out, which was one of the quickest methods. DPPH is a stable free radical and could accept hydrogen and electron from the donors accompanying with a color change from purple to yellow. The antioxidant activities of the synthesized AgNPs by *Cornus officinalis* extract were evaluated against DPPH at different concentrations as shown in Fig. 6. The AgNPs displayed a significant scavenging activity against the DPPH, which increased in a dose-dependent manner and had scavenging activities of 78.3% in  $12.5 \mu\text{g mL}^{-1}$  of AgNPs. With the continuous increase of AgNPs to  $100.0 \mu\text{g mL}^{-1}$ , the scavenging activities of AgNPs did not have obvious changes. The DPPH scavenging activity of AgNPs is basically similar with previously reports by KÜP<sup>40</sup> and Kivcak,<sup>41</sup> indicating that AgNPs synthesized by *Cornus officinalis* extract could be used in treatment of many diseases caused by oxidative stress.

#### Antimicrobial activities of biosynthesized AgNPs

We selected both Gram positive bacteria *S. aureus* and Gram negative bacteria *E. coli* to evaluate the antimicrobial activity of the biosynthesized AgNPs. Fig. 7 showed the absorbance at 600 nm for these two pathogens at different AgNPs doses



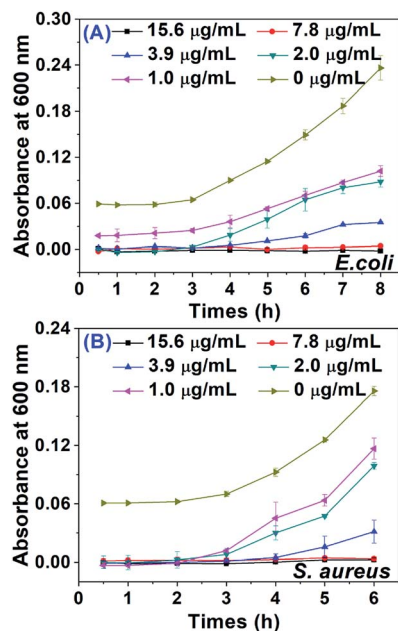


Fig. 7 The antimicrobial activity of biosynthesized AgNPs for (A) *E. coli* and (B) *S. aureus*.

plotted over a few hours, where the AgNPs exhibited potential dose-dependent antimicrobial activity against both pathogens. Even in low AgNPs doses, the growth of both pathogens was obviously inhibited. The minimum inhibition concentrations (MIC) were obtained both to be  $7.8 \mu\text{g mL}^{-1}$  for *S. aureus* and *E. coli*. In minimum inhibition concentration, both *S. aureus* and *E. coli* could be effectively inhibited within 8.0 h and 6.0 h, respectively, as shown in Fig. 7. The MIC values for both *S. aureus* and *E. coli* are basically similar with the results reported by He and his coworkers that the AgNPs biosynthesized by using lotus extract with an average size of  $12.9 \pm 3.7 \text{ nm}$  also had an obvious inhibitive effect for *S. aureus* with MIC  $10 \mu\text{g mL}^{-1}$ .<sup>36</sup> At the same time, we also noticed that the biosynthesized AgNPs using leaf extract of *Aesculus hippocastanum* by KÜP and his coworkers with an average size  $50.0 \pm 5.0 \text{ nm}$  exhibited more superior antimicrobial effects for *S. aureus* and *E. coli* both with MIC  $1.56 \mu\text{g mL}^{-1}$ .<sup>40</sup> Otherwise, the biosynthesized AgNPs with average size  $45 \text{ nm}$  using *Lactobacillus brevis* isolated from Chinese koumiss displayed MIC values of  $8.2 \mu\text{g mL}^{-1}$ ,  $12.5 \mu\text{g mL}^{-1}$  against *E. coli* and *S. aureus*, respectively.<sup>7</sup> It seems that the antimicrobial activity of biosynthesized AgNPs have an ambiguous relationship with the size. We speculated the difference of antimicrobial activity among the AgNPs biosynthesized by different plant extracts might arise from active constituents of extract, which could attach to the surface of AgNPs and may have significant effect on AgNPs adherence to the negatively charged bacterial cell wall or the affinity of AgNPs for phosphorous and sulfur-containing compounds on the cell.

### Internalization of biosynthesized AgNPs

We carried out the flow cytometric analysis to assess the internalization of AgNPs in bacteria according to the method of Suzuki using light scattering principles.<sup>33</sup> Earlier reports are

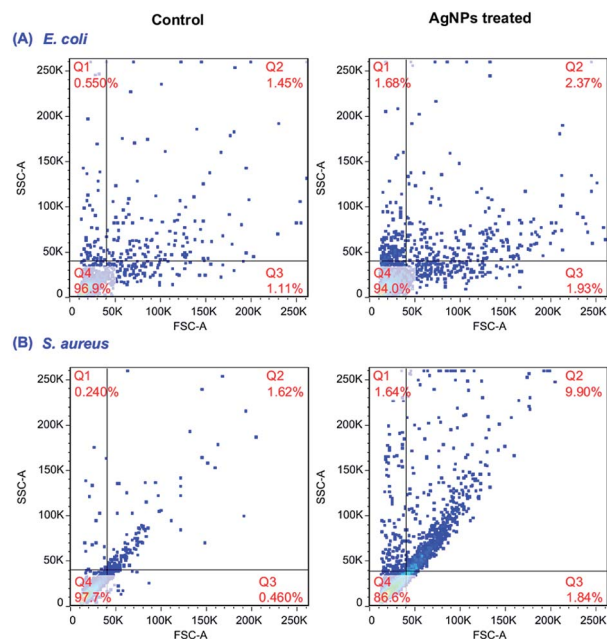


Fig. 8 AgNPs uptake analysis in (A) *E. coli*; (B) *S. aureus* assessed by flow cytometry.

available that as the presence of granules in cytoplasm, granulocytes could scatter more light in  $90^\circ$  directions. This is hypothesized that the internalized NPs in bacterial cells could act as granules and scatter more lights.<sup>42</sup> There was a significant increase in side scatter (SSC) value for both *S. aureus* and *E. coli* as shown in Fig. 8, indicating the internalization of biosynthesized AgNPs.

### Anticancer activities of biosynthesized AgNPs

By exposing AgNPs with concentration in the range of  $0$  to  $100.0 \mu\text{g mL}^{-1}$  to three cancer cell lines including HCT116, SW620 and HepG2 for 24 h, the anticancer activities of biosynthesized AgNPs were preliminarily assessed. The MTT assay was used to determine the cytotoxicity of biosynthesized AgNPs for these cancer cell lines and the results were shown in Fig. 9. It was found that the reduction of cell viability for AgNPs treated cancer cell lines occurred in a dose-dependent fashion. The AgNPs exposed cell viability significantly decreases with increased doses of AgNPs. In the cases of HCT116 and HepG2 cell lines, cell viability was significantly decreased to 25.2% and 8.6% at  $100.0 \mu\text{g mL}^{-1}$  of AgNPs doses, respectively. However, the toxicity effect of biosynthesized AgNPs for SW620 cancer cell line was much poorer comparing with other two cancer cell lines. The slight reduction of cell viabilities to 81.4% were observed in SW620 cancer cell at the doses of AgNPs  $100.0 \mu\text{g mL}^{-1}$ , meaning a poor anticancer activities of biosynthesized AgNPs for SW620 cell lines. The  $\text{IC}_{50}$  values of AgNPs against HCT116 and HepG2 were determined using the GraphPad Prism 8.0 software package. It was found that the  $\text{IC}_{50}$  values of the biosynthesized AgNPs were  $20.68$  and  $69.72 \mu\text{g mL}^{-1}$  for HCT116 and HepG2 cancer cell lines, respectively. These results indicated that the AgNPs synthesized by *Cornus officinalis*



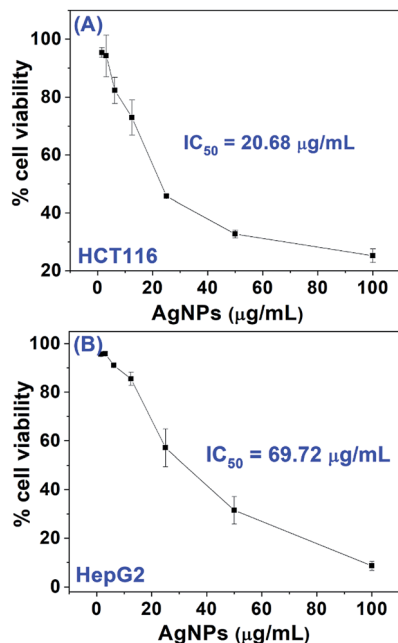


Fig. 9 Inhibition effects of biosynthesized AgNPs on (A) HCT116 and (B) HepG2.

extract under 365 nm UV radiation could be a promising candidate for anticancer drugs. Here, the  $IC_{50}$  value of biosynthesized AgNPs by us for HepG2 cancer cell lines showed distinct cytotoxicity comparing with He and his coworkers using *Cornus officinalis* extract at alkaline ( $21.46 \mu\text{g mL}^{-1}$ ),<sup>29</sup> which may originate from the bioactive compounds covered in the surface of biosynthesized AgNPs.

Although nanoparticles have attracted particular attention to diagnose and treat cancer in the last two decades, the interaction mechanism between nanoparticles and cell remains elusive to a large extent. Studies have shown that AgNPs synthesized by traditional medicine extract with anticancer effect, such as *Iresine herbstii*,<sup>43</sup> *Sesbania grandiflora*<sup>6</sup> and *Alpinia katsumadai*<sup>44</sup> would have superior cytotoxic effects against cancer cell lines like Hela, MCF-7 and GES-1. These results may give us enlightenment for reasonable design of the antineoplastic based on AgNPs synthesized by plant extract.

## Conclusions

We present herein a systematically evaluation of the biosynthesis parameters, such as UV radiation, pH of extract, material proportion and reaction times, on the AgNPs formation and size in green synthesis of AgNPs by utilizing *Cornus officinalis* extract. The results revealed that UV radiation could influence both the formation yield and the average size of AgNPs below pH 7.0, and the size of AgNPs was sensitive to pH of extract, material proportion. The size, shape and surface properties of the AgNPs so-prepared were further characterized by X-ray diffraction (XRD), transmission electron microscopy (TEM) and dynamic light scattering (DLS), revealing a face-centered cubic (fcc) structure and both spherical and polygonal shape

with average particle size of  $64.5 \pm 0.3 \text{ nm}$  covered by anion (zeta potential:  $-24.8 \text{ mV}$ ). By calculating the free radical scavenging rate for DPPH, the antioxidant activities of AgNPs were assessing. When the concentration of AgNPs increased to  $12.5 \mu\text{g mL}^{-1}$ , the free radical scavenging rate was 78.3% meaning a good antioxidant activity. The biosynthesized AgNPs by *Cornus officinalis* extract revealed superior inhibition activities for the growth of *E. coli* and *S. aureus*, where the MIC values were both  $7.8 \mu\text{g mL}^{-1}$ . The uptake of AgNPs inside the bacterial cell was confirmed using flow cytometric analysis by measuring the SSC values. Furthermore, the biosynthesized AgNPs also displayed significant anticancer activities for HCT116 and HepG2 cell lines with  $IC_{50}$  values of 20.68 and  $69.72 \mu\text{g mL}^{-1}$ , respectively, indicating a superior anticancer activity. But no obvious cytotoxicity even at  $100.0 \mu\text{g mL}^{-1}$  was observed against SW620 cell line. These results confirmed that the biosynthesis parameters on the green synthesis of AgNPs by using *Cornus Officinalis* extract also played pivotal roles in the size and morphology and so-prepared AgNPs might be useful for the development of new alternative antioxidant, antimicrobial and anticancer agents in biomedicine.

## Conflicts of interest

There are no conflicts to declare.

## Acknowledgements

This work was financially supported by the National Natural Science Foundation of China (Grant No. 21705029); the Young Talent fund of University Association for Science and Technology in Shaanxi, China (Grant No. 20190307) and the Fundamental Research Funds for the Central Universities, CHD (Grant No. 300102120303).

## Notes and references

- H. Kang, J. T. Buchman, R. S. Rodriguez, H. L. Ring, J. He, K. C. Bantz and C. L. Haynes, Stabilization of Silver and Gold Nanoparticles: Preservation and Improvement of Plasmonic Functionalities, *Chem. Rev.*, 2019, **119**, 664–699.
- S. Eckhardt, P. S. Brunetto, J. Gagnon, M. Priebe, B. Giese and K. M. Fromm, Nanobio Silver: Its Interactions with Peptides and Bacteria, and Its Uses in Medicine, *Chem. Rev.*, 2013, **113**, 4708–4754.
- Y. Chen, Z. Fan, Z. Zhang, W. Niu, C. Li, N. Yang, B. Chen and H. Zhang, Two-Dimensional Metal Nanomaterials: Synthesis, Properties, and Applications, *Chem. Rev.*, 2018, **118**, 6409–6455.
- H. D. Beyene, A. A. Werkneh, H. K. Bezabh and T. G. Ambaye, Synthesis paradigm and applications of silver nanoparticles (AgNPs), a review, *Sustainable Mater. Technol.*, 2017, **13**, 18–23.
- S. H. Lee and B. H. Jun, Silver Nanoparticles: Synthesis and Application for Nanomedicine, *Int. J. Mol. Sci.*, 2019, **20**, 24.
- M. Jeyaraj, G. Sathishkumar, G. Sivanandhan, D. MubarakAli, M. Rajesh, R. Arun, G. Kapildev,





- M. Manickavasagam, N. Thajuddin, K. Premkumar and A. Ganapathi, Biogenic silver nanoparticles for cancer treatment: An experimental report, *Colloids Surf., B*, 2013, **106**, 86–92.
- 7 M. S. Riaz Rajoka, H. M. Mehwish, H. Zhang, M. Ashraf, H. Fang, X. Zeng, Y. Wu, M. Khurshid, L. Zhao and Z. He, Antibacterial and antioxidant activity of exopolysaccharide mediated silver nanoparticle synthesized by *Lactobacillus brevis* isolated from Chinese koumiss, *Colloids Surf., B*, 2020, **186**, 110734.
- 8 L. Y. Wei, J. R. Lu, H. Z. Xu, A. Patel, Z. S. Chen and G. F. Chen, Silver nanoparticles: synthesis, properties, and therapeutic applications, *Drug Discovery Today*, 2015, **20**, 595–601.
- 9 M. G. Casagrande and R. de Lima, Synthesis of Silver Nanoparticles Mediated by Fungi: A Review, *Frontiers in Bioengineering and Biotechnology*, 2019, **7**, 16.
- 10 M. Yadi, E. Mostafavi, B. Saleh, S. Davaran, I. Aliyeva, R. Khalilov, M. Nikzamid, N. Nikzamid, A. Akbarzadeh, Y. Panahi and M. Milani, Current developments in green synthesis of metallic nanoparticles using plant extracts: a review, *Artif. Cells, Nanomed., Biotechnol.*, 2018, 1–8.
- 11 N. Tarannum, D. Divya and Y. K. Gautam, Facile green synthesis and applications of silver nanoparticles: a state-of-the-art review, *RSC Adv.*, 2019, **9**, 34926–34948.
- 12 A. Roy, O. Bulut, S. Some, A. K. Mandal and M. D. Yilmaz, Green synthesis of silver nanoparticles: biomolecule-nanoparticle organizations targeting antimicrobial activity, *RSC Adv.*, 2019, **9**, 2673–2702.
- 13 X. X. Zhao, L. F. Zhou, M. S. R. Rajoka, L. Yan, C. M. Jiang, D. Y. Shao, J. Zhu, J. L. Shi, Q. S. Huang, H. Yang and M. L. Jin, Fungal silver nanoparticles: synthesis, application and challenges, *Crit. Rev. Biotechnol.*, 2018, **38**, 817–835.
- 14 H. E. Emam and H. B. Ahmed, Polysaccharides templates for assembly of nanosilver, *Carbohydr. Polym.*, 2016, **135**, 300–307.
- 15 C. Dipankar and S. Murugan, The green synthesis, characterization and evaluation of the biological activities of silver nanoparticles synthesized from *Iresine herbstii* leaf aqueous extracts, *Colloids Surf., B*, 2012, **98**, 112–119.
- 16 S. Khan, S. Singh, S. Gaikwad, N. Nawani, M. Junnarkar and S. V. Pawar, Optimization of process parameters for the synthesis of silver nanoparticles from *Piper betle* leaf aqueous extract, and evaluation of their antiphytofungic activity, *Environ. Sci. Pollut. Res. Int.*, 2020, **27**, 27221–27233.
- 17 R. Heydari and M. Rashidipour, Green synthesis of silver nanoparticles using extract of oak fruit hull (jaft): synthesis and in vitro cytotoxic effect on mcf-7 cells, *Int. J. Breast Cancer*, 2015, **2015**, 846743.
- 18 G. Premanand, N. Shanmugam, N. Kannadasan, K. Sathishkumar and G. Viruthagiri, *Nelumbo nucifera* leaf extract mediated synthesis of silver nanoparticles and their antimicrobial properties against some human pathogens, *Appl. Nanosci.*, 2016, **6**, 409–415.
- 19 T. V. M. Sreekanth, S. Ravikumar and I. Y. Eom, Green synthesized silver nanoparticles using *Nelumbo nucifera* root extract for efficient protein binding, antioxidant and cytotoxicity activities, *J. Photochem. Photobiol., B*, 2014, **141**, 100–105.
- 20 A. Verma and M. S. Mehata, Controllable synthesis of silver nanoparticles using *Neem* leaves and their antimicrobial activity, *J. Radiat. Res. Appl. Sci.*, 2016, **9**, 109–115.
- 21 C. Yu, J. C. Tang, X. M. Liu, X. W. Ren, M. N. Zhen and L. Wang, Green Biosynthesis of Silver Nanoparticles Using *Eriobotrya japonica* (Thunb.) Leaf Extract for Reductive Catalysis, *Materials*, 2019, **12**, 12.
- 22 V. Dhand, L. Soumya, S. Bharadwaj, S. Chakra, D. Bhatt and B. Sreedhar, Green synthesis of silver nanoparticles using *Coffea arabica* seed extract and its antibacterial activity, *Mater. Sci. Eng., C*, 2016, **58**, 36–43.
- 23 S. Wei, Y. Wang, Z. Tang, J. Hu, S. Rui, L. Jingjie, Z. Tuan, H. Guo, W. Nan and X. Rongrong, A Size-Controlled Green Synthesis of Silver Nanoparticles by the Berry Extract of Sea Buckthorn and the Biological Activities, *New J. Chem.*, 2020, **44**, 9304–9312.
- 24 M. H. Lin, H. K. Liu, W. J. Huang, C. C. Huang, T. H. Wu and F. L. Hsu, Evaluation of the Potential Hypoglycemic and Beta-Cell Protective Constituents Isolated from *Corni Fructus* To Tackle Insulin-Dependent Diabetes Mellitus, *J. Agric. Food Chem.*, 2011, **59**, 7743–7751.
- 25 W. Ma, K. J. Wang, C. S. Cheng, G. Q. Yan, W. L. Lu, J. F. Ge, Y. X. Cheng and N. Li, Bioactive compounds from *Cornus officinalis* fruits and their effects on diabetic nephropathy, *J. Ethnopharmacol.*, 2014, **153**, 840–845.
- 26 T. Sozanski, A. Z. Kucharska, A. Rapak, D. Szumny, M. Trocha, A. Merwid-Lad, S. Dzimira, T. Piasecki, N. Piorecki, J. Magdalan and A. Szelag, Iridoid-loganic acid versus anthocyanins from the *Cornus mas* fruits (cornelian cherry): Common and different effects on diet-induced atherosclerosis, PPARs expression and inflammation, *Atherosclerosis*, 2016, **254**, 151–160.
- 27 M. S. Stanković and M. D. Topuzović, In vitro antioxidant activity of extracts from leaves and fruits of common dogwood (*Cornus sanguinea*L.), *Acta Bot. Gallica*, 2012, **159**, 79–83.
- 28 A. E. Sharp-Tawfik, A. M. Coiner, C. B. MarElia, M. Kazantzis, C. Zhang and B. R. Burkhardt, Compositional analysis and biological characterization of *Cornus officinalis* on human 1.1B4 pancreatic beta cells, *Mol. Cell. Endocrinol.*, 2019, **494**, 8.
- 29 Y. He, X. Li, J. Wang, Q. Yang, B. Yao, Y. Zhao, A. Zhao, W. Sun and Q. Zhang, Synthesis, characterization and evaluation cytotoxic activity of silver nanoparticles synthesized by Chinese herbal *Cornus officinalis* via environment friendly approach, *Environ. Toxicol. Pharmacol.*, 2017, **56**, 56–60.
- 30 G. Kaur, A. Kalia and H. S. Sodhi, Size controlled, time-efficient biosynthesis of silver nanoparticles from *Pleurotus florida* using ultra-violet, visible range, and microwave radiations, *Inorg. Nano-Met. Chem.*, 2020, **50**, 35–41.
- 31 H. Liu, H. Zhang, J. Wang and J. Wei, Effect of temperature on the size of biosynthesized silver nanoparticle: Deep



- insight into microscopic kinetics analysis, *Arabian J. Chem.*, 2020, **13**, 1011–1019.
- 32 M. Sathishkumar, K. Sneha, S. W. Won, C. W. Cho, S. Kim and Y. S. Yun, Cinnamon zeylanicum bark extract and powder mediated green synthesis of nano-crystalline silver particles and its bactericidal activity, *Colloids Surf., B*, 2009, **73**, 332–338.
- 33 H. Suzuki, T. Toyooka and Y. Ibuki, Simple and Easy Method to Evaluate Uptake Potential of Nanoparticles in Mammalian Cells Using a Flow Cytometric Light Scatter Analysis, *Environ. Sci. Technol.*, 2007, **41**, 3018–3024.
- 34 E. Friehs, Y. AlSalka, R. Jonczyk, A. Lavrentieva, A. Jochums, J. G. Walter, F. Stahl, T. Scheper and D. Bahnemann, Toxicity, phototoxicity and biocidal activity of nanoparticles employed in photocatalysis, *J. Photochem. Photobiol. C Photochem. Rev.*, 2016, **29**, 1–28.
- 35 P. Mondal, K. Schwinn and M. Huix-Rotllant, Impact of the redox state of flavin chromophores on the UV-vis spectra, redox and acidity constants and electron affinities, *J. Photochem. Photobiol., A*, 2020, **387**, 9.
- 36 Y. He, X. Li, Y. Zheng, Z. Wang, Z. Ma, Q. Yang, B. Yao, Y. Zhao and H. Zhang, A green approach for synthesizing silver nanoparticles, and their antibacterial and cytotoxic activities, *New J. Chem.*, 2018, **42**, 2882–2888.
- 37 N. Manosalva, G. Tortella, M. C. Diez, H. Schalchli, A. B. Seabra, N. Duran and O. Rubilar, Green synthesis of silver nanoparticles: effect of synthesis reaction parameters on antimicrobial activity, *World J. Microbiol. Biotechnol.*, 2019, **35**, 9.
- 38 P. Fernando, M. J. Piao, A. X. Zhen, M. J. Ahn, J. M. Yi, Y. H. Choi and J. W. Hyun, Extract of *Cornus officinalis* Protects Keratinocytes from Particulate Matter-induced Oxidative Stress, *Int. J. Med. Sci.*, 2020, **17**, 63–70.
- 39 B. Kumar, K. Smita and L. Cumbal, Biosynthesis of silver nanoparticles using lavender leaf and their applications for catalytic, sensing, and antioxidant activities, *Nanotechnol. Rev.*, 2016, **5**, 521–528.
- 40 F. O. Kup, S. Coskuncay and F. Duman, Biosynthesis of silver nanoparticles using leaf extract of *Aesculus hippocastanum* (horse chestnut): Evaluation of their antibacterial, antioxidant and drug release system activities, *Mater. Sci. Eng., C*, 2020, **107**, 11.
- 41 T. Fafal, P. Taştan, B. S. Tüzün, M. Ozyazici and B. Kivcak, Synthesis, characterization and studies on antioxidant activity of silver nanoparticles using *Asphodelus aestivus* Brot. aerial part extract, *South Afr. J. Bot.*, 2017, **112**, 346–353.
- 42 M. Kumari, S. Shukla, S. Pandey, V. P. Giri, A. Bhatia, T. Tripathi, P. Kakkar, C. S. Nautiyal and A. Mishra, Enhanced Cellular Internalization: A Bactericidal Mechanism More Relative to Biogenic Nanoparticles than Chemical Counterparts, *ACS Appl. Mater. Interfaces*, 2017, **9**, 4519–4533.
- 43 C. Dipankar and S. Murugan, The green synthesis, characterization and evaluation of the biological activities of silver nanoparticles synthesized from *Iresine herbstii* leaf aqueous extracts, *Colloids Surf., B*, 2012, **98**, 112–119.
- 44 Y. Q. He, F. F. Wei, Z. Y. Ma, H. Zhang, Q. Yang, B. H. Yao, Z. R. Huang, J. Li, C. Zeng and Q. Zhang, Green synthesis of silver nanoparticles using seed extract of *Alpinia katsumadai*, and their antioxidant, cytotoxicity, and antibacterial activities, *RSC Adv.*, 2017, **7**, 39842–39851.

